Journal of Quality Measurement and Analysis
Jurnal Pengukuran Kualiti dan Analisis

JQMA 10(2) 2014, 51-63

STABILITY ANALYSIS OF STAGNATION-POINT FLOW PAST A SHRINKING SHEET IN A NANOFLUID

(Analisis Kestabilan bagi Aliran Titik-Genangan melalui Helaian Mengecut dalam Nanobendalir)

AMIN NOOR[1], ROSLINDA NAZAR[1] & KHAMISAH JAFAR[2]

ABSTRACT

In this paper, a numerical and theoretical study has been performed for the stagnation-point boundary layer flow and heat transfer towards a shrinking sheet in a nanofluid. The mathematical nanofluid model in which the effect of the nanoparticle volume fraction is taken into account, is considered. The governing nonlinear partial differential equations are transformed into a system of nonlinear ordinary differential equations using a similarity transformation which is then solved numerically using the function bvp4c in Matlab. Numerical results are obtained for the skin friction coefficient, the local Nusselt number as well as the velocity and temperature profiles for some values of the governing parameters, namely the nanoparticle volume fraction ϕ, the shrinking parameter λ and the Prandtl number Pr. Three different types of nanoparticles are considered, namely Cu, Al_2O_3 and TiO_2. It is found that solutions do not exist for larger shrinking rates and dual (upper and lower branch) solutions exist when $\lambda < -1.0$. A stability analysis has been performed to determine which branch solutions are stable and physically realisable. It is also found that the upper branch solutions are stable while the lower branch solutions are unstable.

Keywords: heat transfer; nanofluid; shrinking sheet; stability analysis; stagnation-point flow

ABSTRAK

Dalam makalah ini, kajian secara teori dan berangka telah dilakukan bagi aliran lapisan sempadan titik-genangan dan pemindahan haba terhadap helaian mengecut dalam nanobendalir. Model nanobendalir bermatematik dengan mengambil kira kesan pecahan isi padu nanozarah telah dipertimbangkan. Persamaan pembezaan separa menakluk tak linear dijelmakan kepada suatu sistem persamaan pembezaan biasa tak linear menggunakan penjelmaan keserupaan yang kemudiannya diselesaikan secara berangka dengan fungsi bvp4c dalam Matlab. Keputusan berangka diperoleh bagi pekali geseran kulit, nombor Nusselt setempat, serta profil-profil halaju dan suhu bagi beberapa nilai parameter menakluk seperti pecahan isi padu nanozarah ϕ, parameter mengecut λ dan nombor Prandtl Pr. Tiga jenis nanozarah berbeza yang dipertimbangkan adalah Cu, Al_2O_3 dan TiO_2. Didapati bahawa penyelesaian tidak wujud bagi kadar pengecutan yang lebih besar dan penyelesaian dual (cabang atas dan bawah) wujud apabila $\lambda < -1.0$. Analisis kestabilan dilakukan bagi menentukan penyelesaian cabang yang stabil dan bermakna secara fizikal. Didapati juga bahawa penyelesaian cabang atas adalah stabil manakala penyelesaian cabang bawah tidak stabil.

Kata kunci: pemindahan haba; nanobendalir; helaian mengecut; analisis kestabilan; aliran titik-genangan

1. Introduction

Heat transfer is an important process in physics and engineering, and consequently improvements in heat transfer characteristics will improve the efficiency of many processes. Nanofluid is a new class of heat transfer fluids that comprise of a base fluid and nanoparticles. The use of additive is a technique applied to enhance the heat transfer performance of base fluids. Nanofluids have been shown to increase the thermal conductivity and convective

heat transfer performance of the base liquid (Abu-Nada 2008). Thus nanofluids have many applications in industry such as coolants, lubricants, heat exchangers, micro channel heat sinks and many others. The innovative technique, which uses a suspension of nanoparticles in the base fluid, was first introduced by Choi (1995) in order to develop advanced heat transfer fluids with substantially higher conductivities. There have been many studies in the literature to better understand the mechanism behind the enhanced heat transfer characteristics. An excellent collection of papers on this topic can be found in the books by Das *et al*. (2007) and in some review papers, for example, by Buongiorno (2006), Wang and Mujumdar (2007), and Kakaç and Pramuanjaroenkij (2009). Therefore, quite many investigators have studied the flow and thermal characteristics of nanofluids, both theoretically and experimentally.

For the flow over a shrinking sheet, the fluid is attracted towards a slot and as a result it shows quite different characteristics from the stretching case. From a physical point of view, vorticity generated at the shrinking sheet is not confined within a boundary layer and a steady flow is not possible unless either a stagnation flow or adequate suction is applied at the sheet. As discussed by Goldstein (1965), this new type of shrinking flow is essentially a backward flow. Miklavčič and Wang (2006) were the first who have investigated the flow over a shrinking sheet with suction effect. Steady two-dimensional and axisymmetric boundary layer stagnation point flow and heat transfer towards a shrinking sheet was analysed by Wang (2008). Thereafter various aspects of stagnation point flow and heat transfer over a shrinking sheet were investigated by many authors (Fang 2008; Fang *et al*. 2009; Ishak *et al*. 2010; Lok *et al*. 2011; Bhattacharyya 2011; Bhattacharyya *et al*. 2011; Nazar *et al*. 2011; Jafar *et al.* 2013). All studies mentioned above refer to the stagnation-point flow towards a stretching/ shrinking sheet in a viscous and Newtonian fluid. Bachok *et al*. (2011) investigated the effects of solid volume fraction and the type of the nanoparticles on the fluid flow and heat transfer characteristics of a nanofluid over a stretching/shrinking sheet. On the other hand, Tham *et al*. (2012) considered the steady mixed convection boundary layer flow near the lower stagnation-point of a horizontal circular cylinder with a constant surface temperature embedded in a porous medium saturated by a nanofluid containing gyrotactic microorganisms.

In this paper, the steady stagnation-point flow towards a shrinking sheet in a nanofluid is theoretically studied. Three different types of nanoparticles, namely copper (Cu), alumina (Al_2O_3) and titania (TiO_2) are considered. The nanofluid equations model as proposed by Tiwari and Das (2007) has been used. Although similar problem has been investigated, the main objective of the present paper is to extend the work of Nazar *et al*. (2011) by performing stability analysis of the dual solutions in order to determine which solution is stable and physically realisable.

2. Governing Equations

We consider the steady two-dimensional stagnation-point flow of a nanofluid past a shrinking sheet with the linear velocity $u_w(x) = cx$, and the velocity of the far (inviscid) flow is $u_e(x) = ax$, where a and c are constant, and x is the coordinate measured along the shrinking surface. The flow takes place at $y \geq 0$, where y is the coordinate measured normal to the shrinking surface. It is also assumed that the surface of the shrinking sheet is subjected to a prescribed temperature $T_w(x) = T_\infty + bx$, where T_∞ is the temperature of the ambient nanofluid, and b is a constant with $b > 0$ (heated shrinking sheet). A steady uniform stress leading to equal and opposite forces is applied along the $x-$axis so that the sheet is stretched, keeping the origin fixed in a nanofluid.

The basic conservation of mass, momentum and energy equations for a nanofluid in Cartesian coordinates x and y are given by (Tiwari & Das 2007; Nazar *et al.* 2011)

$$\frac{\partial u}{\partial x}+\frac{\partial v}{\partial y}=0 \tag{1}$$

$$\frac{\partial u}{\partial t}+u\frac{\partial u}{\partial x}+v\frac{\partial u}{\partial y}=-\frac{1}{\rho_{nf}}\frac{\partial p}{\partial x}+\frac{\mu_{nf}}{\rho_{nf}}\left(\frac{\partial^2 u}{\partial x^2}+\frac{\partial^2 u}{\partial y^2}\right) \tag{2}$$

$$\frac{\partial v}{\partial t}+u\frac{\partial v}{\partial x}+v\frac{\partial v}{\partial y}=-\frac{1}{\rho_{nf}}\frac{\partial p}{\partial y}+\frac{\mu_{nf}}{\rho_{nf}}\left(\frac{\partial^2 v}{\partial x^2}+\frac{\partial^2 v}{\partial y^2}\right) \tag{3}$$

$$\frac{\partial T}{\partial t}+u\frac{\partial T}{\partial x}+v\frac{\partial T}{\partial y}=\alpha_{nf}\left(\frac{\partial^2 T}{\partial x^2}+\frac{\partial^2 T}{\partial y^2}\right) \tag{4}$$

subject to the initial and boundary conditions

$$\begin{aligned} &t<0:\ u=0,\ v=0,\ T=T_\infty \text{ for any } x,\ y\\ &t\geq 0:\ v=0,\ u=u_w(x)=cx,\quad T=T_w(x)\quad \text{at}\quad y=0\\ &\qquad u\to u_e(x)=ax,\quad T\to T_\infty\quad \text{as}\quad y\to\infty \end{aligned} \tag{5}$$

Here u and v are the velocity components along the x and y axes, respectively, T is the temperature of the nanofluid, p is the fluid pressure, α_{nf} is the thermal diffusivity of the nanofluid, μ_{nf} is the effective viscosity of the nanofluid, and ρ_{nf} is the effective density of the nanofluid, which are given by (Oztop & Abu-Nada 2008)

$$\begin{aligned} &\alpha_{nf}=\frac{k_{nf}}{(\rho C_p)_{nf}},\ \mu_{nf}=\frac{\mu_f}{(1-\phi)^{2.5}},\ \rho_{nf}=(1-\phi)\rho_f+\phi\rho_s,\\ &(\rho C_p)_{nf}=(1-\phi)(\rho C_p)_f+\phi(\rho C_p)_s,\ \frac{k_{nf}}{k_f}=\frac{(k_s+2k_f)-2\phi(k_f-k_s)}{(k_s+2k_f)+\phi(k_f-k_s)} \end{aligned} \tag{6}$$

where ϕ is the solid volume fraction of the nanofluid or the nanoparticle volume fraction, ρ_f is the reference density of the fluid fraction, ρ_s is the reference density of the solid fraction, μ_f is the viscosity of the fluid fraction, k_{nf} is the effective thermal conductivity of the nanofluid, k_f is the thermal conductivity of the fluid, k_s is the thermal conductivity of the solid, and $(\rho C_p)_{nf}$ is the heat capacity of the nanofluid.

3. Steady-State Flow Case

We introduce now the following similarity variables:

$$\eta = (a/\nu_f)^{1/2} y, \quad \psi = (a\nu_f)^{1/2} x f(\eta), \\ \theta(\eta) = (T - T_\infty)/(T_w - T_\infty), \tag{7}$$

where ν_f is the kinematic viscosity of the fluid and the stream function ψ is defined in the usual way as $u = \partial\psi/\partial y$ and $v = -\partial\psi/\partial x$, which identically satisfy Eq. (1). On substituting (6) and (7) into Eqs. (2)-(4), we obtain the following nonlinear ordinary differential equations:

$$\varepsilon_1 f''' + f f'' + 1 - f'^2 = 0 \tag{8}$$

$$\frac{1}{\Pr}\varepsilon_2 \theta'' + f\theta' - f'\theta = 0 \tag{9}$$

and the boundary conditions (5) become

$$f(0) = 0, \quad f'(0) = \lambda, \quad \theta(0) = 1 \\ f'(\infty) = 1, \quad \theta(\infty) = 0 \tag{10}$$

where primes denote differentiation with respect to η, $\Pr = \nu_f/\alpha_f$ is the Prandtl number and $\lambda = c/a$ is the stretching/shrinking parameter with $\lambda > 0$ for stretching and $\lambda < 0$ for shrinking. Meanwhile ε_1 and ε_2 are two constants relating to the properties of the nanofluid, defined by

$$\varepsilon_1 = \frac{1}{(1-\phi)^{2.5}\left(1-\phi+\phi\rho_s/\rho_f\right)}, \\ \varepsilon_2 = \frac{k_{nf}/k_f}{(1-\phi)+\phi(\rho C_p)_s/(\rho C_p)_f} \tag{11}$$

The pressure p can be determined from Eq. (3) as

$$p = p_0 - \rho_{nf} a^2 x^2/2 - \rho_{nf} v^2/2 + \mu_{nf}\partial v/\partial y \tag{12}$$

where p_0 p_0 is the stagnation pressure. It is worth mentioning that Eqs. (8) and (9) reduce to those first derived by Wang (2008) when the nanoparticle volume fraction parameter $\phi = 0$ (regular Newtonian fluid), and Pr = 1.

The quantities of practical interest in this study are the skin friction coefficient at the surface of the shrinking sheet C_f and the local Nusselt number Nu_x, which can easily shown to be given by

$$\mathrm{Re}_x^{1/2} C_f = \frac{1}{(1-\phi)^{2.5}} f''(0), \quad \mathrm{Re}_x^{-1/2} Nu_x = -\frac{k_{nf}}{k_f}\theta'(0) \tag{13}$$

where $\mathrm{Re}_x = u_e(x)x/\nu_f$ is the local Reynolds number.

4. Stability Analysis

It has been shown in some papers (Weidman *et al*. 2006; Roşca & Pop 2013) that dual (lower and upper branch) solutions exist. In order to determine which of these solutions are physically realisable in practice, a stability analysis of Eqs. (8)-(10) is necessary. Following Weidman *et al*. (2006), a dimensionless time variable τ has to be introduced. The use of τ is associated with an initial value problem and this is consistent with the question of which solution will be obtained in practice (physically realisable). Thus, the new variables for the unsteady problem are

$$\begin{aligned} &\psi = (a\nu_f)^{1/2} x f(\eta,\tau), \quad \theta(\eta,\tau) = (T - T_\infty)/(T_w - T_\infty), \\ &\eta = (a/\nu_f)^{1/2} y, \ \tau = at \end{aligned} \tag{14}$$

Substituting (14) into (2)-(4), we obtain

$$\varepsilon_1 \frac{\partial^3 f}{\partial \eta^3} + f\frac{\partial^2 f}{\partial \eta^2} + 1 - \left(\frac{\partial f}{\partial \eta}\right)^2 - \frac{\partial^2 f}{\partial \eta \partial \tau} = 0 \tag{15}$$

$$\frac{\varepsilon_2}{\Pr}\frac{\partial^2 \theta}{\partial \eta^2} + f\frac{\partial \theta}{\partial \eta} - \frac{\partial f}{\partial \eta}\theta - \frac{\partial \theta}{\partial \tau} = 0 \tag{16}$$

subject to the boundary conditions

$$\begin{aligned} &f(0,\tau) = 0, \quad \frac{\partial f}{\partial \eta}(0,\tau) = \lambda, \quad \theta(0,\tau) = 1 \\ &\frac{\partial f}{\partial \eta}(\eta,\tau) \to 1, \quad \theta(\eta,\tau) \to 0 \text{ as } \eta \to \infty \end{aligned} \tag{17}$$

To determine the stability of the solution $f = f_0(\eta)$ and $\theta = \theta_0(\eta)$ satisfying the boundary-value problem (8)-(10), we write (Weidman *et al*. 2006; Roşca & Pop 2013)

$$\begin{aligned} &f(\eta,\tau) = f_0(\eta) + e^{-\gamma\tau} F(\eta,\tau), \\ &\theta(\eta,\tau) = \theta_0(\eta) + e^{-\gamma\tau} S(\eta,\tau), \end{aligned} \tag{18}$$

where γ is an unknown eigenvalue parameter, while $F(\eta,\tau)$ and $S(\eta,\tau)$ are small relative to $f_0(\eta)$ and $\theta_0(\eta)$. Substituting (18) into (15) and (16), we obtain the following linearised problem:

$$\varepsilon_1 \frac{\partial^3 F}{\partial \eta^3} + f_0\frac{\partial^2 F}{\partial \eta^2} + Ff_0'' - 2f_0'\frac{\partial F}{\partial \eta} + \gamma\frac{\partial F}{\partial \eta} - \frac{\partial^2 F}{\partial \eta \partial \tau} = 0 \tag{19}$$

$$\frac{\varepsilon_2}{\Pr}\frac{\partial^2 S}{\partial \eta^2} + f_0\frac{\partial S}{\partial \eta} + F\theta_0' - f_0'S - \frac{\partial F}{\partial \eta}\theta_0 + \gamma S - \frac{\partial S}{\partial \tau} = 0 \tag{20}$$

subject to the boundary conditions

$$F(0,\tau)=0,\quad \frac{\partial F}{\partial \eta}(0,\tau)=0,\quad S(0,\tau)=0$$
$$\frac{\partial F}{\partial \eta}(\eta,\tau)\to 0,\quad S(\eta,\tau)\to 0 \text{ as } \eta\to\infty \tag{21}$$

As suggested by Weidman *et al*. (2006), we investigate the stability of the steady flow and heat transfer solution $f_0(\eta)$ and $\theta_0(\eta)$ by setting $\tau=0$, and hence $F=F_0(\eta)$ and $S=S_0(\eta)$ in (19) and (20) to identify initial growth or decay of the solution (18). To test our numerical procedure we have to solve the following linear eigenvalue problem:

$$\varepsilon_1 F_0'''+f_0F_0''+F_0f_0''-2f_0'F_0'+\gamma F_0'=0 \tag{22}$$

$$\frac{\varepsilon_2}{\Pr}S_0''+f_0S_0'+F_0\theta_0'-f_0'S_0-F_0'\theta_0+\gamma S_0=0 \tag{23}$$

with the boundary conditions

$$F_0(0)=0,\quad F_0'(0)=0,\quad S_0(0)=0$$
$$F_0'(\eta)\to 0,\quad S_0(\eta)\to 0 \text{ as } \eta\to\infty \tag{24}$$

It should be mentioned that for particular values of λ,θ, and other parameters involved, the corresponding steady flow solution $f_0(\eta)$ and $\theta_0(\eta)$, the stability of the steady flow solution is determined by the smallest eigenvalue γ_1. According to Harris *et al*. (2009), the range of possible eigenvalues can be determined by relaxing a boundary condition on $F_0'(\eta)$ or $S_0(\eta)$. For the present problem, we relax the condition that $F'_0(\eta)\to 0$ as $\eta\to\infty$ and for a fixed value of γ we solve the system (22-23) along with the new boundary condition $F_0''(0)=1$.

5. Results and Discussion

The system of nonlinear ordinary differential equations (8) and (9) subject to the boundary conditions (10) are solved numerically using the bvp4c function in Matlab. Following Oztop and Abu-Nada (2008), we considered the range of nanoparticle volume fraction to be $0\le\phi\le 0.2$. The Prandtl numbers Pr considered in this study are Pr = 1 (for comparison) and Pr = 6.2 (water-based nanofluid). Further, it should also be pointed out that the thermophysical properties of fluid and nanoparticles (Cu, Al_2O_3, TiO_2) used in this study are given in Table 1 (Oztop & Abu-Nada 2008).

On the other hand, it is worth mentioning that the present study reduces to regular (Newtonian) fluid when $\phi=0$. The dual (first and second) solutions are obtained by setting different initial guesses for the missing values of $f''(0)$ and $\theta'(0)$, where all profiles satisfy the far field boundary conditions (10) asymptotically. In order to validate the present numerical method used, we have compared our results with those obtained by Nazar *et al.* (2011) for various values of the shrinking parameter ($\lambda<0$) when $\phi=0.2$ and Pr = 1 as shown in Tables 2 and 3. Table 2 presents the values of the skin friction coefficient $\mathrm{Re_x}^{1/2}C_f$ while

Table 3 illustrates the values of the local Nusselt number $\mathrm{Re}_x^{-1/2} Nu_x$ for shrinking sheets. The comparisons with Nazar *et al.* (2011) are found to be in excellent agreement. Therefore, the present numerical solution is further validated, so that we are confident our results are accurate. Further, Tables 2 and 3 also present the numerical values for the present problem in nanofluid with different nanoparticles (Cu, Al_2O_3, TiO_2) for various nanoparticle volume fraction ϕ.

Table 1: Thermophysical properties of fluids and nanoparticles (Oztop & Abu-Nada 2008)

Physical properties	Fluid phase (water)	Cu	Al_2O_3	TiO_2
C_p (J/kg K)	4179	385	765	686.2
ρ (kg/m^3)	997.1	8933	3970	4250
k (W/mK)	0.613	400	40	8.9538

Table 2: Value of $\mathrm{Re}_x^{1/2} C_f$ for shrinking sheet $(\lambda < 0)$ with $\phi = 0.2$ (results in [ ] are those of Nazar *et al*. (2011))

λ	Upper branch			Lower branch		
	Cu	Al_2O_3	TiO_2	Cu	Al_2O_3	TiO_2
-0.25	2.98374	2.34163	2.38247	-	-	-
	[2.98374]	[2.34163]	[2.38247]	[-]	[-]	[-]
-0.50	3.18254	2.49765	2.54121	-	-	-
	[3.18254]	[2.49765]	[2.54121]	[-]	[-]	[-]
-0.75	3.16898	2.48701	2.53038	-	-	-
	[3.16898]	[2.48701]	[2.53038]	[-]	[-]	[-]
-1.00	2.82750	2.21902	2.25772	-	-	-
	[2.82750]	[2.21902]	[2.25772]	[-]	[-]	[-]
-1.10	2.52506	1.98166	2.01622	0.10475	0.08221	0.08364
	[2.52506]	[1.98166]	[2.01622]	[0.10475]	[0.08221]	[0.08364]
-1.15	2.30281	1.80724	1.83876	0.24832	0.19488	0.19828
	[2.30281]	[1.80724]	[1.83876]	[0.24832]	[0.19488]	[0.19828]
-1.20	1.98415	1.55716	1.58432	0.49717	0.39018	0.39698
	[1.98415]	[1.55716]	[1.58431]	[0.49717]	[0.39018]	[0.39698]

Table 3: Value of $\mathrm{Re}_x^{-1/2} Nu_x$ for shrinking sheet $(\lambda < 0)$ with $\phi = 0.2$ and Pr=1
(results in [ ] are those of Nazar *et al*. (2011))

λ	Upper branch			Lower branch		
	Cu	Al_2O_3	TiO_2	Cu	Al_2O_3	TiO_2
-0.25	1.03949	0.93681	0.89501	-	-	-
	[1.03949]	[0.93681]	[0.89501]	[-]	[-]	[-]
-0.50	0.87555	0.75219	0.71593	-	-	-
	[0.87555]	[0.75219]	[0.71593]	[-]	[-]	[-]
-0.75	0.67521	0.52533	0.49578	-	-	-
	[0.67521]	[0.52533]	[0.49578]	[-]	[-]	[-]
-1.00	0.40000	0.21058	0.19002	-	-	-
	[0.40000]	[0.21058]	[0.19002]	[-]	[-]	[-]
-1.10	0.23996	0.02522	0.00975	-2.28730	-3.46470	-3.42839
	[0.23996]	[0.02522]	[0.00975]	[-2.27462]	[-3.46468]	[-3.42772]

to be continued...

.....continuation

-1.15	0.13343	-0.09941	-0.11156	-1.51080	-2.27652	-2.25087
	[0.13343]	[-0.09941]	[-0.11156]	[-1.51080]	[-2.27652]	[-2.25086]
-1.20	-0.01501	-0.27512	-0.28277	-1.01271	-1.55706	-1.53989
	[-0.01501]	[-0.27512]	[-0.28277]	[-1.01270]	[-1.55706]	[-1.15162]

It is shown in Tables 2 and 3 the variations of the skin friction coefficient $\mathrm{Re}_x^{1/2} C_f$ and the local Nusselt number $\mathrm{Re}_x^{-1/2} Nu_x$, respectively, with $\lambda < 0$ (shrinking sheet) for different nanoparticles (Cu, Al_2O_3, TiO_2) when $\phi = 0.2$. As can be seen clearly in Figures 1 to 4, it is found that dual solutions exist when $\lambda < -1$, up to a certain critical value of λ, say λ_c, beyond which the boundary layer separates from the surface, thus no solution is obtained. In this study, the value of λ_c is found to be $\lambda_c = 1.2465$, which is consistent with the value obtained in Nazar *et al*. (2011) and Wang (2008) for $\phi = 0$ (regular Newtonian fluid). We identify the upper (first) and lower (second) branch solutions in the following discussion by how they appear in Figures 1 to 4, i.e. the upper branch solution has higher values for a given λ than the lower branch solution. It is also shown in Figures 1 and 2 that for a particular nanoparticle used (Cu as in example), as the nanoparticle volume fraction ϕ increases, the skin friction coefficient and the local Nusselt number also increase.

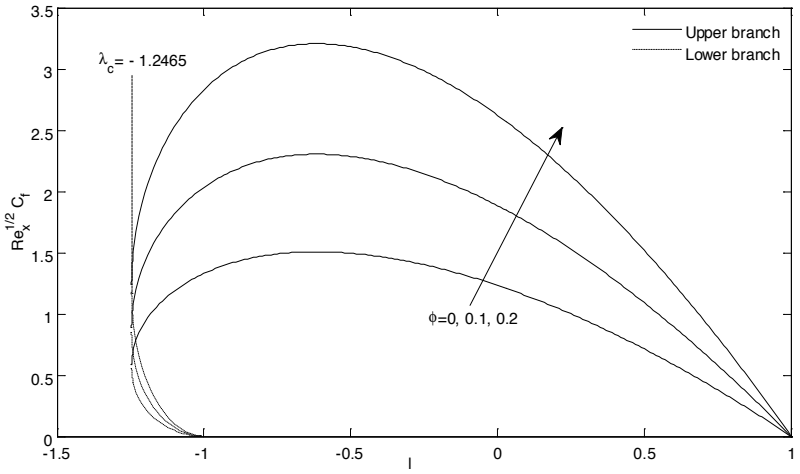

Figure 1: Variation of the skin friction coefficient $\mathrm{Re}_x^{1/2} C_f$ with λ for different value of ϕ in Cu-water nanofluid

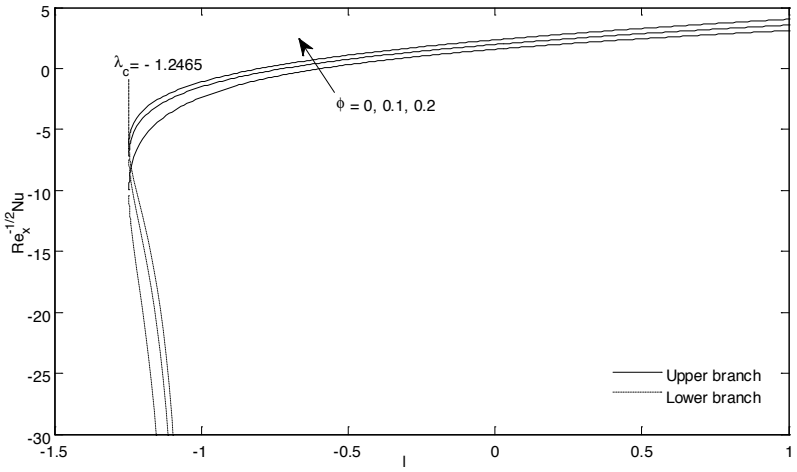

Figure 2: Variation of the local Nusselt number $\mathrm{Re}_x^{-1/2} Nu_x$ with λ for different value of ϕ in Cu-water nanofluid when Pr = 6.2

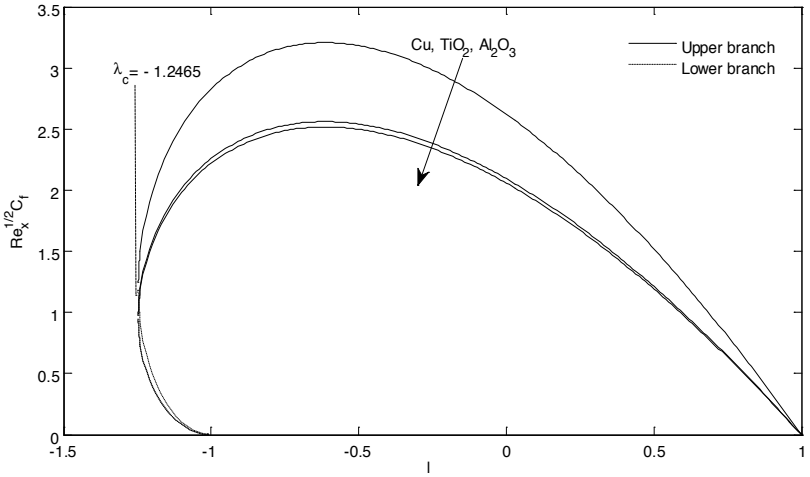

Figure 3: Variation of the skin friction coefficient $\mathrm{Re}_x^{1/2} C_f$ with λ for different types of nanoparticle when $\phi = 0.2$

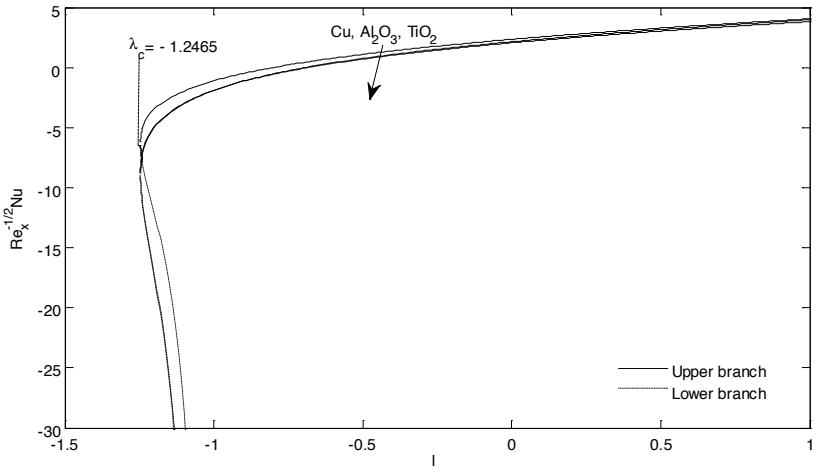

Figure 4: Variation of the local Nusselt number $\mathrm{Re}_x^{-1/2} Nu_x$ with λ for different types of nanoparticle when $\phi = 0.2$ and Pr = 6.2

On the other hand, Figures 3 and 4 show that for a fixed value of ϕ, say $\phi = 0.2$, the skin friction is highest for nanoparticle Cu (nanoparticle with high density), followed by TiO_2 and Al_2O_3, while the local Nusselt number is largest for Cu, followed by Al_2O_3 and TiO_2 (nanoparticle with low thermal conductivity). Figure 5 displays the velocity profiles $f'(\eta)$ for nanoparticles Cu, Al_2O_3 and TiO_2 when $\phi = 0.2$ and λ = -1.2 (shrinking sheet), while Figure 6 illustrates the corresponding temperature profiles when Pr = 6.2. The velocity and temperature profiles for Al_2O_3 and TiO_2 are almost identical while the velocity for nanoparticle Cu is the highest but the temperature for Cu is the lowest. This is consistent with the variation of the reduced skin friction coefficient $f''(0)$ which is highest for Cu and the variation of the temperature gradient or heat transfer rate $-\theta'(0)$ which is highest for TiO_2. Therefore, it is found that nanoparticles with low thermal conductivity, TiO_2, have better enhancement on heat transfer compared to Al_2O_3 and Cu. These velocity and temperature profiles in Figures 5 and 6 support the existence of dual nature of the solutions presented in Figures 1 to 4. It is seen that the lower branch solutions have larger boundary layer thickness compared to the upper branch solutions. These profiles satisfy the far field boundary conditions (10) asymptotically, which support the numerical results obtained and thus, cannot be neglected mathematically.

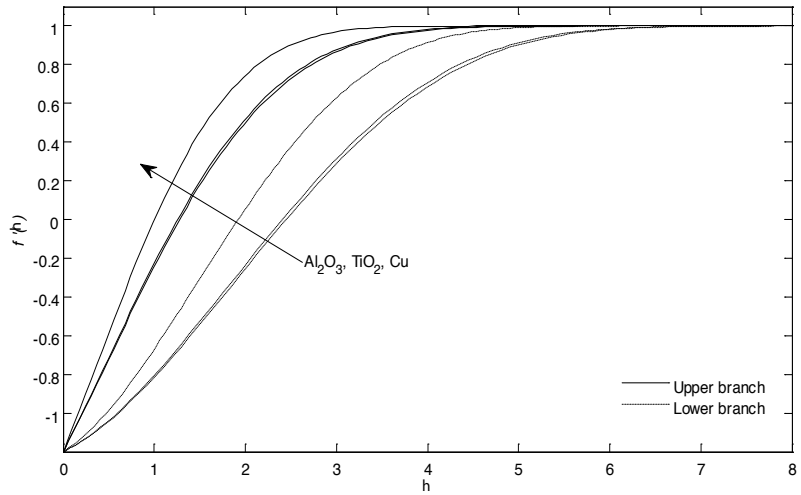

Figure 5: Velocity profiles $f'(\eta)$ for different types of nanoparticle when $\phi = 0.2$ and λ = -1.2 (shrinking sheet)

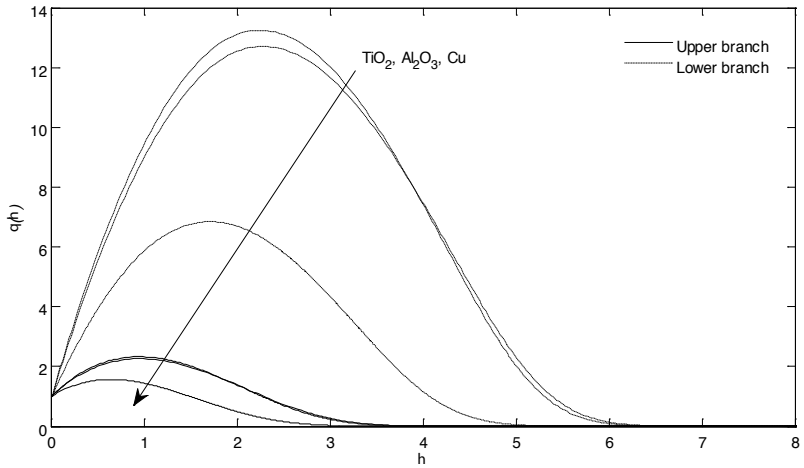

Figure 6: Temperature profiles $\theta(\eta)$ for different types of nanoparticle when ϕ= 0.2, λ = -1.2 (shrinking sheet) and Pr = 6.2

We can expect that the upper branch solution is stable, while the lower branch solution is not, since the upper branch is the only solution for the case $\lambda \geq -1$. In order to validate this, a stability analysis is carried out by solving linear eigenvalue problem (22-23) subject to homogeneous boundary conditions (24). The smallest eigenvalue γ_1 for some values of ϕ and λ are shown in Table 4 when Pr = 6.2 for different type of nanoparticles. The results show that all the upper branch solutions have positive eigenvalue γ_1 while all the lower branch solutions have negative eigenvalue γ_1. We conclude that the upper branch solution is physically realisable (stable) while the lower branch is not physically realisable (unstable) over time. Notice that the smallest eigenvalue γ_1 is unique when different types of nanoparticles or different nanoparticle volume fraction parameters ϕ are used since these parameters do not affect the critical value λ_c as shown in Figures 1 to 4, due to the uncoupled Eqs. (8) and (9). We can also expect the same observation when different Prandtl number Pr is used.

Table 4: Value of smallest eigenvalue γ_1 for some value of ϕ and λ

ϕ	λ	Upper branch			Lower branch		
		Cu	Al_2O_3	TiO_2	Cu	Al_2O_3	TiO_2
0.1	-1.05	1.2180	1.2180	1.2180	-0.9363	-0.9363	-0.9363
	-1.10	1.0463	1.0463	1.0463	-0.8437	-0.8437	-0.8437
	-1.15	0.8429	0.8429	0.8429	-0.7135	-0.7135	-0.7135
	-1.20	0.5780	0.5780	0.5780	-0.5172	-0.5172	-0.5172
	-1.24	0.2121	0.2121	0.2121	-0.2036	-0.2036	-0.2036
0.2	-1.05	1.2180	1.2180	1.2180	-0.9363	-0.9363	-0.9363
	-1.10	1.0463	1.0463	1.0463	-0.8437	-0.8437	-0.8437
	-1.15	0.8429	0.8429	0.8429	-0.7135	-0.7135	-0.7135
	-1.20	0.5780	0.5780	0.5780	-0.5172	-0.5172	-0.5172
	-1.24	0.2121	0.2121	0.2121	-0.2036	-0.2036	-0.2036

6. Conclusions

We have studied numerically the problem of steady two-dimensional laminar stagnation-point flow towards a shrinking sheet in nanofluids. The governing partial differential equations are transformed into nonlinear ordinary differential equations via the similarity transformation, before being solved numerically using bvp4c function in Matlab. The comparison of the results with previously published results shows an excellent agreement thus gives us confidence in our computations presented in this paper. Numerical results were obtained for the skin friction coefficient, the local Nusselt number as well as the velocity and temperature profiles for some values of the governing parameters, namely the nanoparticle volume fraction ϕ ($0 \le \phi \le 0.2$), the shrinking parameter λ and the Prandtl number Pr. It was found that nanoparticles with low thermal conductivity (TiO_2) have better enhancement on heat transfer compared to those with higher thermal conductivity (Al_2O_3 and Cu). For a particular nanoparticle, skin friction coefficient and the heat transfer rate at the surface increased as the nanoparticle volume fraction ϕ increased. It was also found that solutions do not exist for larger shrinking rates and dual solutions exist when $\lambda < -1.0$ for both a regular fluid ($\phi = 0$) and for a nanofluid ($\phi \neq 0$). The stability analysis was performed and showed that the upper branch solution is stable while the lower branch solution is unstable.

Acknowledgement

This work was supported by the research grant (AP-2013-009) from the Universiti Kebangsaan Malaysia.

References

Abu-Nada E. 2008. Application of nanofluids for heat transfer enhancement of separated flows encountered in a backward facing step. *Int. J. Heat Fluid Flow* **29**: 242-249.

Bachok N., Ishak A. & Pop I. 2011. Stagnation-point flow over a stretching/shrinking sheet in a nanofluid *Nanoscale Res. Lett.* **6**: Article ID 623 (10 pages).

Bhattacharyya K., Mukhopadhyay S. & Layek G.C. 2011. Effects of suction/blowing on steady boundary layer stagnation-point flow and heat transfer towards a shrinking sheet with thermal radiation. *Int. J. Heat Mass Transfer* **54**: 302-307.

Bhattacharyya K. 2011. Dual solutions in boundary layer stagnation-point flow and mass transfer with chemical reaction past a stretching/shrinking sheet. *Int. Comm. Heat Mass Transfer* **38**: 917-922.
Buongiorno J. 2006. Convective transport in nanofluids. *ASME J. Heat Transfer* **128**: 240-250.
Choi S.U.S. 1995. Enhancing thermal conductivity of fluids with nanoparticles. In: D.A. Siginer and H.P. Wang (eds.), Development and Applications of non-Newtonian Flows. *ASME MD-vol. 231 and FED-vol. 66*, pp. 99-105
Das S.K., Choi S.U.S., Yu W. & Pradeep T. 2007. *Nanofluids: Science and Technology*. Hoboken: Wiley.
Fang T. 2008. Boundary layer flow over a shrinking sheet with power-law velocity. *Int. J. Heat Mass Transfer* **51**: 5838-5843.
Fang T., Zhang J. & Yao S. 2009. Viscous flow over an unsteady shrinking sheet with mass transfer. *Chin. Phys. Lett.* **26**: 014703.
Goldstein S. 1965. On backward boundary layers and flow in converging passages. *J. Fluid Mech*. **21**: 33-45.
Harris S.D., Ingham D.B. & Pop I. 2009. Mixed convection boundary-layer flow near the stagnation point on a vertical surface in a porous medium: Brinkman model with slip. *Trans. Porous Media* **77**: 267-285.
Ishak A., Lok Y.Y. & Pop I. 2010. Stagnation-point flow over a shrinking sheet in a micropolar fluid. *Chem. Eng. Commun.* **197**: 1417-1427.
Jafar K., Ishak A. & Nazar R. 2013. MHD stagnation-point flow over a nonlinearly stretching/shrinking sheet. *J. Aerosp. Eng.* **26**: 829-834.
Kakaç S. & Pramuanjaroenkij A. 2009. Review of convective heat transfer enhancement with nanofluids. *Int. J. Heat Mass Transfer* **52**: 3187-3196.
Lok Y.Y., Ishak A. & Pop I. 2011. MHD stagnation-point flow towards a shrinking sheet. *Int. J. Numer. Methods Heat Fluid Flow* **21**: 61-72.
Miklavčič M. & Wang C.Y. 2006. Viscous flow due to a shrinking sheet. *Quart. Appl. Math.* **64**: 283-290.
Nazar R., Jaradat M., Arifin N. M. & Pop I. 2011. Stagnation-point flow past a shrinking sheet in a nanofluid. *Cen. Eur. J. Phys.* **9**(5): 1195-1202.
Oztop H.F. & Abu-Nada E. 2008. Numerical study of natural convection in partially heated rectangular enclosures filled with nanofluids. *Int. J. Heat Fluid Flow* **29**: 1326-1336.
Roşca A.V. & Pop I. 2013. Flow and heat transfer over a vertical permeable stretching/shrinking sheet with a second order slip. *Int. J. Heat Mass Transfer* **60**: 355-364.
Tham L.Y.S., Nazar R. & Pop I. 2012. Mixed convection flow at the lower stagnation point of a circular cylinder embedded in a porous medium filled by a nanofluid containing gyrotactic microorganisms. *J. Quality Measurement & Analysis* **8**(2): 45-63.
Tiwari R.J. & Das M.K. 2007. Heat transfer augmentation in a two-sided lid-driven differentially heated square cavity utilizing nanofluids. *Int. J. Heat Mass Transfer* **50**: 2002-2018.
Wang C.Y. 2008. Stagnation flow towards a shrinking sheet. *Int. J. Non-Linear Mech.* **43**: 377-382.
Wang X.-Q. & Mujumdar A.S. 2007. Heat transfer characteristics of nanofluids: a review. *Int. J. Thermal Sci.* **46**: 1-19.
Weidman P.D., Kubittschek D.G. & Davis A.M.J. 2006. The effect of transpiration on self-similar boundary layer flow over moving surfaces. *Int. J. Engng. Sci.* **44**: 730-737.

[1]*School of Mathematical Sciences*
Faculty of Science & Technology
Universiti Kebangsaan Malaysia
43600 UKM Bangi
Selangor DE, MALAYSIA
*E-mail: mamn.ukm@gmail.com, rmn@ukm.edu.my**

[2]*Faculty of Engineering & Built Environment*
Universiti Kebangsaan Malaysia
43600 UKM Bangi
Selangor DE, MALAYSIA
E-mail: kjafar61@gmail.com

* Corresponding author